



RESEARCH ARTICLE

10.1029/2019JA027331

Comparison of Van Allen Probes Energetic Electron Data With Corresponding GOES-15 Measurements: 2012–2018

Key Points:

- Comparison of operational GOES data with NASA science data
- Statistical study of radiation belt properties over 6 years
- Study shows radial range and energy range where GOES can monitor radiation belts

D. N. Baker¹ , H. Zhao¹ , X. Li¹ , S. G. Kanekal² , A. N. Jaynes³ , B. T. Kress^{4,5}, J. V. Rodriguez^{4,5} , H. J. Singer⁶ , S. G. Claudepierre^{7,8} , J. F. Fennell⁷ , and V. Hoxie¹

¹Laboratory for Atmospheric and Space Physics, University of Colorado Boulder, Boulder, CO, USA, ²NASA Goddard Space Flight Center, Greenbelt, MD, USA, ³Department of Physics and Astronomy, University of Iowa, Iowa City, IA, USA, ⁴Cooperative Institute for Research in Environmental Sciences, University of Colorado Boulder, Boulder, CO, USA, ⁵National Centers for Environmental Information, Boulder, CO, USA, ⁶Space Weather Prediction Center, NOAA, Boulder, CO, USA, ⁷The Aerospace Corporation, El Segundo, CA, USA, ⁸Department of Atmospheric and Oceanic Sciences, University of California, Los Angeles, CA, USA

Correspondence to:

D. N. Baker,
daniel.baker@lasp.colorado.edu

Citation:

Baker, D. N., Zhao, H., Li, X., Kanekal, S. G., Jaynes, A. N., Kress, B. T., et al. (2019). Comparison of Van Allen Probes Energetic Electron Data with corresponding GOES-15 Measurements: 2012–2018. *Journal of Geophysical Research: Space Physics*, 124, 9924–9942. <https://doi.org/10.1029/2019JA027331>

Received 26 AUG 2019

Accepted 31 OCT 2019

Accepted article online 30 NOV 2019

Published online 04 DEC 2019

Abstract Electron fluxes (especially at energies $E > 0.8$ and 2 MeV) have been measured for many years by sensors on board the Geostationary Operational Environmental Satellite (GOES). These long-term data (nominally at $L \sim 6.6$) have become a mainstay for monitoring the Earth's radiation environment. We have carried out a study directly comparing the comprehensive radiation belt particle measurements from the National Aeronautics and Space Administration dual-spacecraft Van Allen Probes (Radiation Belt Storm Probes) sensor systems with selected GOES operational data. The Van Allen Probes have measured the properties of radiation belt electrons virtually continuously from September 2012 to 2018. We make statistical comparisons of Van Allen Probes electron data near $L = 6$ with concurrent daily averages of equivalent GOES-15 flux values. We also compare Van Allen Probes data at various other L values and at a much broader range of particle energies with the more limited baseline GOES-15 values. These comparisons inform us about the relative calibrations between the scientific and operational systems and also allow us to assess how well GOES data correlate with radiation belt behavior well away from the geostationary orbit location. We find that GOES daily average flux values can be a factor of 100 (or more) below the corresponding Van Allen Probes daily averaged fluxes at $L = 6.0$. This is due to the fact that GOES at stationary orbit often has excursions over large ranges of L space during a given day and strong radial gradients exist in this region of the magnetosphere. These results indicate that it is crucial to augment geosynchronous GOES observations with observations in the core of the outer belt ($L \lesssim 5.0$).

1. Introduction

The geostationary orbit is one of the most heavily employed locations in near-Earth space for communication, reconnaissance, remote sensing, and other applications. At this special equatorial position ($r = 6.6$ Earth radii [R_E] geocentric distance), an orbiting spacecraft circles the Earth once each day and thereby remains fixed above a given spot on Earth's surface. The geostationary Earth orbit (GEO) has therefore become a prized location for both civilian, as well as national security, operational purposes (and has remained so for decades). The U.S. National Oceanic and Atmospheric Administration (NOAA) has flown a dedicated series of Geostationary Operational Environmental Satellite (GOES) missions at key GEO locations since the 1970s. These GOES spacecraft have returned a variety of remote sensing and imaging data pertaining to Earth's surface, oceans, and atmosphere. Especially notable are the GOES global weather images that have informed atmospheric monitoring and modeling for over nearly five decades (Singer et al., 1996). Such GOES data have been crucial for space weather applications (e.g., Baker & Lanzerotti, 2016). Of similarly great importance have been the GOES measurements of in situ energetic particles and magnetic fields along with concurrent data about the Sun (Ackerman et al., 2019; Singer et al., 1996).

In many studies, some dating back decades (e.g., Baker, et al., 1986; Onsager et al., 2004), GEO data have been taken as essentially a surrogate for overall radiation belt properties. When assessing space weather behavior at (or very near) GEO, this can be a reasonable assumption. But in recent times, more and more Earth-orbiting spacecraft have been operating in orbits at middle-Earth orbit (MEO) altitudes and, of course, there are literally hundreds of spacecraft operating in low-Earth orbit (LEO) as well. It is of considerable

©2019. The Authors.

This is an open access article under the terms of the Creative Commons Attribution License, which permits use, distribution and reproduction in any medium, provided the original work is properly cited.

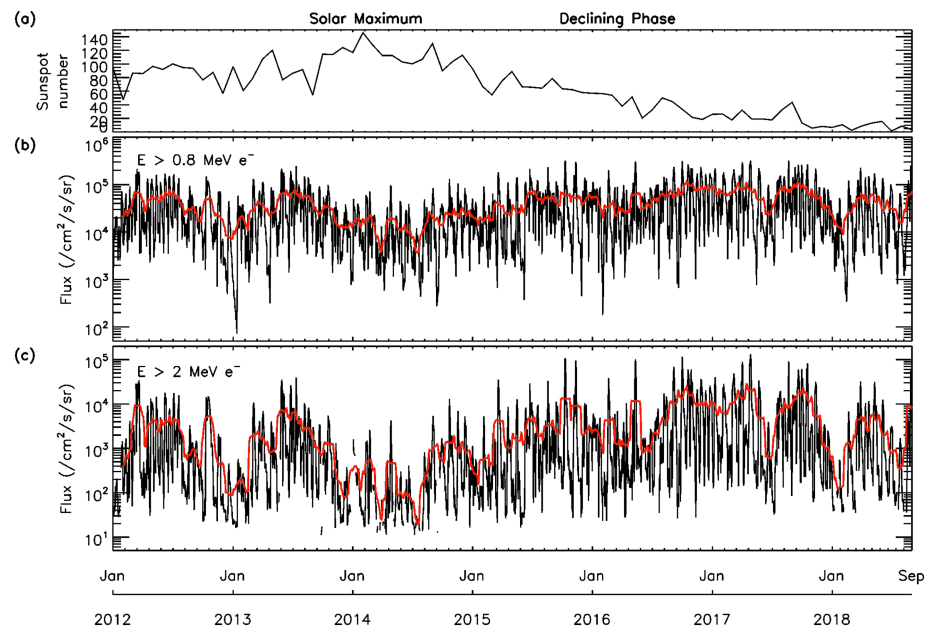


Figure 1. Summary of data for the years 2012 to 2018. (a) The monthly mean sunspot number. (b) Daily flux averages from the GOES-15 spacecraft (black trace) along with the 30-day smoothed average flux (red trace) for the 2012–2018 period for electrons with energy $E > 0.8$ MeV e^- . (c) Similar to (b) but for electrons with $E > 2$ MeV energies.

scientific (and practical) interest, therefore, to assess just how well measurements from a given GEO spacecraft can be used remotely to infer radiation belt properties at various MEO and LEO locations.

The Radiation Belt Storm Probes (RBSP) mission was conceived within National Aeronautics and Space Administration (NASA)'s Living With a Star Program as a comprehensive, dual-spacecraft mission to measure essentially all relevant aspects of the Earth's radiation environment (Mauk et al., 2013). The twin RBSP spacecraft were launched in late August of 2012 and were placed into nearly identical elliptical Earth orbits ($1.1 \times 5.8 R_E$) at $\sim 10^\circ$ inclinations. In November 2012, the RBSP spacecraft were renamed the Van Allen Probes mission and data have been acquired continuously from them since September 2012. Many important—and unexpected—scientific results about the Earth's radiation belts have been obtained with the RBSP measurements, especially from the higher energy electron sensors (Baker et al., 2012; Blake et al., 2013). Features such as the presence of multiple outer Van Allen belts (Baker et al., 2013) and a seeming barrier to inward radial transport of $E \geq 2$ MeV electrons (Baker et al., 2014; Li et al., 2015; Fennell et al., 2015) have been fertile ground for theoretical analysis and modeling (e.g., Ozeke et al., 2018; Thorne et al., 2013).

In this paper, we utilize the Van Allen Probes data to compare with the operational sensor results of a GOES spacecraft. The Van Allen Probes measure across a wide range of differential energy channels, they measure pitch angle distributions, and they cover essentially all relevant L values from $L \sim 1.0$ to beyond $L \sim 6.0$. The Van Allen Probes sensors were extensively calibrated prior to launch in laboratory settings (e.g., Baker et al., 2012) and have also been well modeled using simulation tools (GEANT4). Hence, the Van Allen Probes data can be considered as the “gold standard” against which to compare the more operational GOES measurements.

2. Data Sources and Analysis Methods

The baseline observations for this study come from the Energetic Proton, Electron and Alpha Detector (EPEAD) on board the GOES-15 spacecraft (GOES N Series Data Book, 2010; Hanser, 2011; Rodriguez et al., 2014). This satellite was launched on 4 March 2010 and was subsequently declared operational on 6 December 2011. At that point in time, GOES-15 was adopted by NOAA as the “GOES West” spacecraft at the geographic longitude of 135° W. GOES-15 operated continuously in that position through December of 2018. Hence, we have chosen in this study to use data from the GOES-15 EPEAD “E” sensor from 2012 through 2018. There are two EPEADs on GOES-15, labeled “E” and “W.” In operations, GOES-15

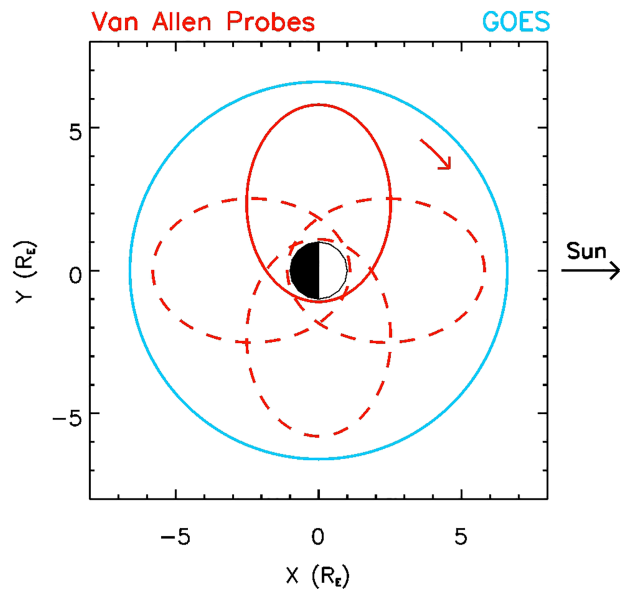


Figure 2. A schematic diagram showing the notional orbits of the GOES and Van Allen Probes spacecraft. The orbits are projected onto the X-Y Geocentric Solar Ecliptic plane. GOES is in a circular orbit at $6.6 R_E$ geocentric, while the Van Allen Probes are in $1.1 \times 5.8 R_E$ elliptical orbits. As indicated by the red dashed ellipses, the Van Allen Probes orbit precesses over time through all local time sectors.

undergoes a yaw flip twice per year. This results in the “E” sensor looking westward when the satellite is upright and eastward when the satellite is inverted (Rodriguez et al, 2014). The >0.8 MeV (E1) and >2 MeV (E2) channel count rates are measured by the EPEAD Dome D3, which has a broad, oblong (35° by 55° half-angle) field-of-view (Hanser, 2011). On-orbit comparisons have demonstrated good agreement between electron measurements by different EPEAD sensors at similar geomagnetic latitudes (Onsager et al., 2004; Meredith et al., 2015). The angular response functions of both the E1 and E2 channels typically span 90 – 100° in pitch angle and are peaked near 90° local pitch angle, although this pitch-angle response varies substantially when the field stretches and a relatively strong east-west magnetic field component

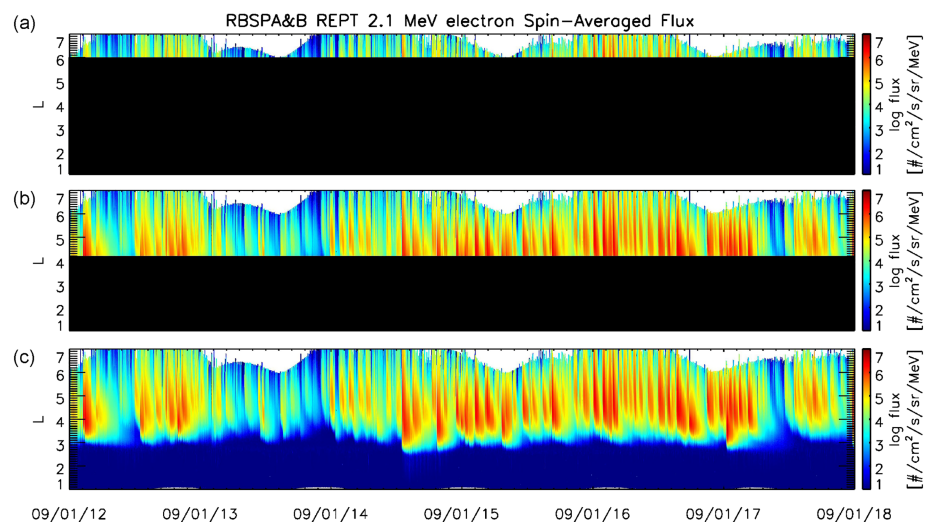


Figure 3. Color-coded differential flux values for electrons with energy $E \sim 2.1$ MeV as measured by instruments on board the Van Allen Probes A and B. The horizontal axis is time from 1 September 2012 to 1 September 2018. The lower panel (c) shows the full measurement set from $L \sim 1$ to $L \sim 7$. (a) Data blocked out (blackened) for $L < 6$ (as described in the text). (b) The same data as in panel (c) but with everything below $L = 4.2$ blocked out. The complete data of panel (c) obviously show temporal and spatial radiation belt features that are not apparent in panels (a) or (b).

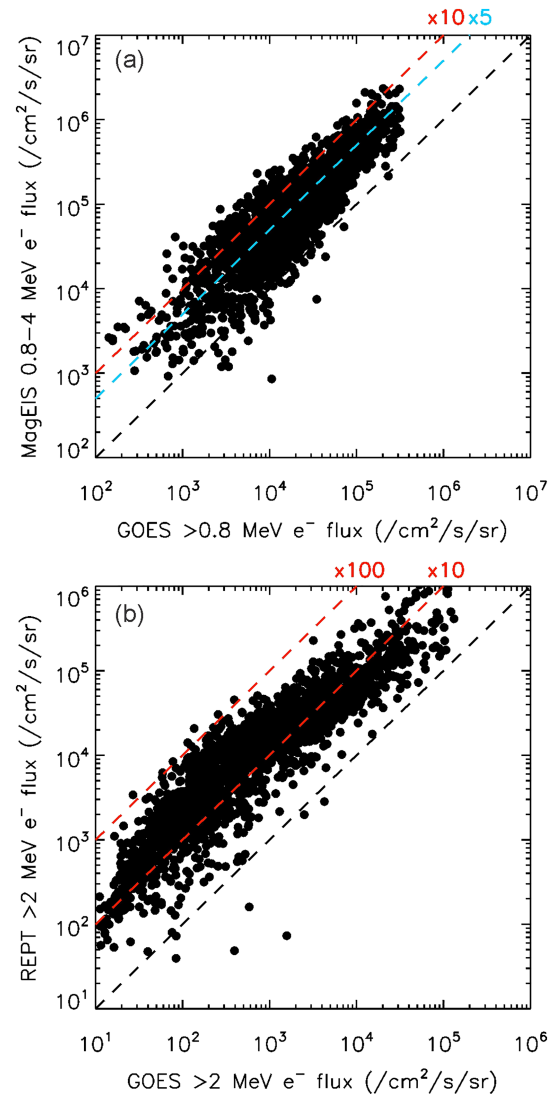


Figure 4. Scatterplots of daily flux averages from the Van Allen Probes at $L = 6$ versus the GOES-15 “E” sensor. (a) Daily values of $E > 0.8$ MeV electrons from Van Allen Probes A versus comparable GOES-15 measurements. (b) Similar to (a) but for electrons with energies $E > 2$ MeV. Data from 1 September 2012 to 1 September 2018 are included in the plots.

develops in the presence of field-aligned currents (Singer et al., 1985; Nagai, 1987). We have not used data from the GOES-15 “W” sensor because, during the last several years, it has exhibited on-orbit degradation with a seasonal and local-time dependence.

For context, Figure 1a shows monthly sunspot numbers (SILSO, 2019) for the period 2012–2018, inclusive. A peak sunspot number of ~ 140 was reached in early 2014. Generally speaking, the period 2012–2014 has been recognized as the “solar maximum” period for Solar Cycle 24. The period from 2015 to the present has been designated as the “declining phase” of Cycle 24 activity. As seen in Figure 1a, the average sunspot number by late 2018 had reached essentially zero indicating the approaching end of Solar Cycle 24 (and the imminent onset of Solar Cycle 25) (Upton, 2018). Figures 1b and 1c show, respectively, the GOES-15 daily averaged integral fluxes of electrons with $E > 0.8$ MeV and $E > 2$ MeV. As seen in Figure 1b, the maximum peak fluxes for 0.8 MeV electrons were observed (briefly) in early 2012 and again in early 2013 and were at a level of $\sim 2 \times 10^5$ electrons $(\text{cm}^2 \text{ s sr})^{-1}$. Such peak fluxes later were regularly met or exceeded in association with recurrent high-speed solar wind streams in the declining solar activity phase during 2015–2017. Overall, the fluxes of $E > 0.8$ MeV electrons ranged typically from $\sim 10^3$ to $\sim 10^5$ $(\text{cm}^2 \text{ s sr})^{-1}$. The red curve in Figure 1b shows the 30-day smoothed flux for this energy range over the analysis period.

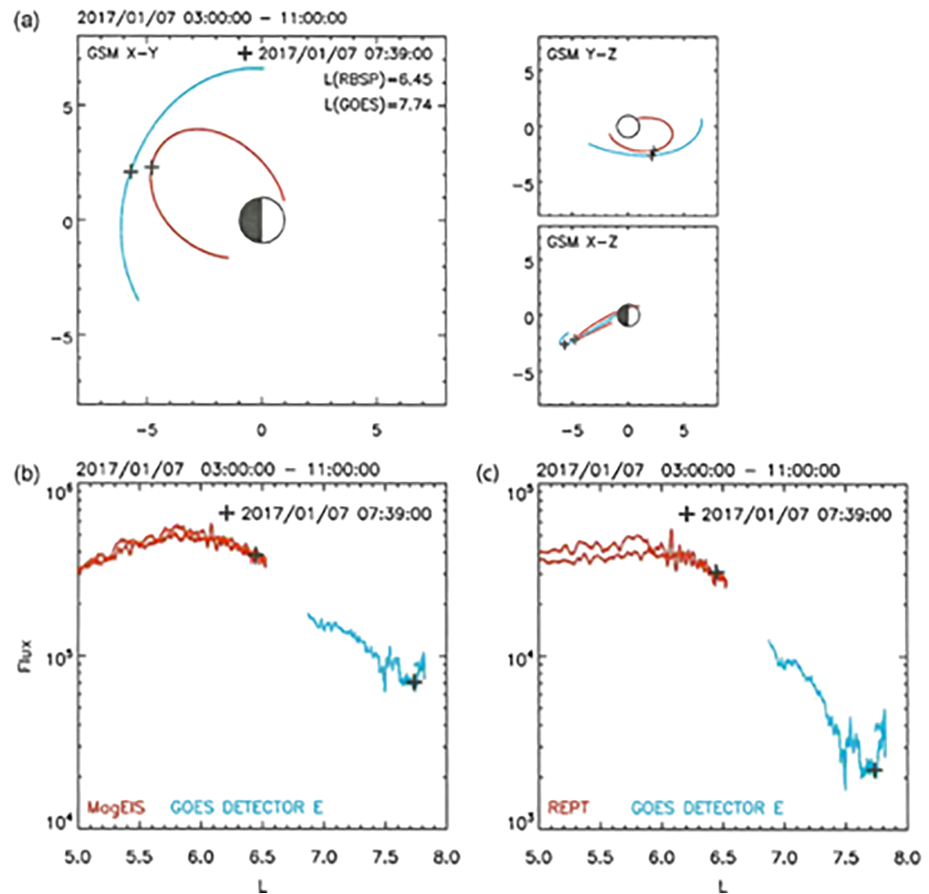


Figure 5. (a) Various orbital projections (as labelled) for the GOES-15 and Van Allen Probes A spacecraft on 7 January 2017. The period covered on this day is 0300 UT to 1100 UT. (b) Fluxes of $E > 0.8$ electrons versus the magnetic shell parameter L for the period 0300–1100 UT on 7 January 2017. Van Allen Probes data are shown in red and GOES-15 data are plotted in blue. The time of closest approach (0739 UT) is shown with the black crosses. (c) Similar to (b) but for electrons with energies $E > 2$ MeV.

Figure 1c shows the daily averaged GOES-15 electron fluxes for $E > 2$ MeV. In general, one observes that the > 2 MeV electrons varied over a wider dynamic range ($\sim 10^1$ to $\sim 10^5$ $\text{cm}^2 \text{ s sr}^{-1}$) and showed more substantial trends (red line) than the corresponding $E > 0.8$ MeV electrons. During the period from late ~ 2013 to the first half of 2014, $E > 2$ MeV electron fluxes were extraordinarily low (see Baker et al., 2019). However, from 2015 to 2018—that is, in the declining sunspot phase—the $E > 2$ MeV electrons regularly peaked above 10^4 electrons $\text{cm}^2 \text{ s sr}^{-1}$. As noted, these relatively high daily average peak fluxes were driven by high-speed solar wind streams emanating from solar coronal holes in the declining sunspot phase of solar activity (Baker et al., 2019).

As shown schematically in Figure 2, the geostationary orbit is equatorial and circular at $6.6 R_E$ geocentric distance. On the other hand, the Van Allen Probes orbits are slightly inclined to the geographic equator ($\sim 10^\circ$) and are highly elliptical ($1.1 \times 5.8 R_E$). Over the course of about 1.5 years, the Van Allen Probes line of apsides precessed completely around the Earth so that the local time of apogee varies widely and systematically (as illustrated in the diagram of Figure 2). When it is recognized that the 10° orbital inclination of the RBS-P spacecraft must be accounted for, the L values sampled by the Van Allen Probes regularly extend to beyond $L \sim 7.0$.

As discussed in the Introduction, GEO measurements as made, for example, by the GOES spacecraft sensors are used to give a portrait of the entire outer Van Allen zone electron population. However, this is not always and completely the case. As an illustration of this, Figure 3 shows measurements from the combined Relativistic Electron-Proton Telescope (REPT) sensors onboard the RBS-P-A and RBS-P-B spacecraft. The

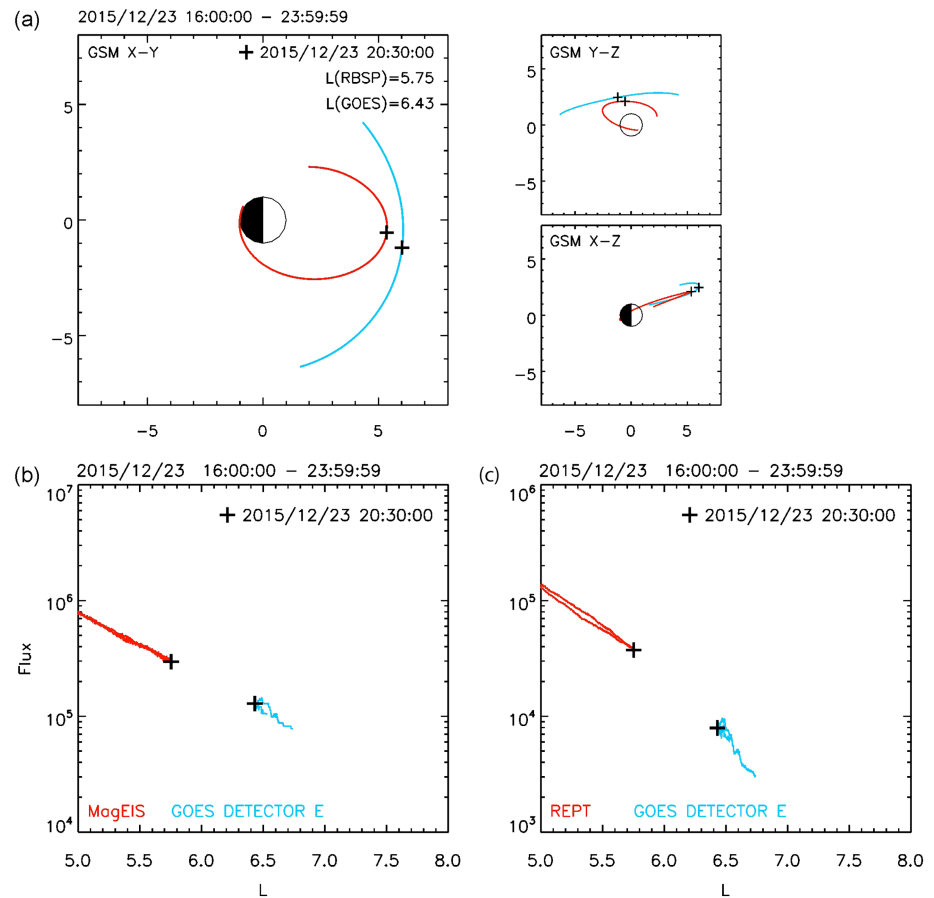


Figure 6. Similar to Figure 5 but for the period 1600–2359 UT on 23 December 2015.

period shown is for 1 September 2012 through 1 September 2018. (This 6-year period has been discussed in some detail by Baker et al., 2019, and Zhao et al., 2019.) The REPT differential energy channel data for $E \sim 2.1$ MeV electrons are presented in the figure as color-coded electron fluxes. (Note that for the Van Allen Probes data shown in this study, we have used Level 2 [spin-averaged] data for daily averaged fluxes. For pitch angle resolved analysis we have used Level 3 data.) The vertical axis in each panel is McIlwain L value calculated based upon the Tsyganenko (1989) magnetic field model. The horizontal axis of the figure shows time from 1 September 2012 to 1 September 2018.

Figure 3a shows the $E = 2.1$ MeV fluxes but with all data below $L = 6.0$ blacked out. Hence, this figure's upper panel shows roughly what a GEO spacecraft detector might be able to sense day-by-day over a 6-year period. Obviously, this view is only the “tip of the iceberg” for the radiation belts. Figure 3b shows a more complete portion of the RBSP data, in this case with only the data below $L = 4.2$ blacked out. Clearly, with the broader swath of data from $4.2 \lesssim L \lesssim 7.0$, one can observe a vast array of outer belt properties including many flux enhancement events and electron losses that only are hinted at in Figure 3a. (Using $L = 4.2$ as the cutoff in Figure 3b was chosen to correspond to the L range that regularly is explored by the Global Positioning Satellite system that carries Los Alamos National Laboratory particle dosimeter detectors (Morley et al., 2016) on board many of the operational constellation's satellites). While sampling at $L \gtrsim 4.2$ reveals much more of the “iceberg” than seen in Figure 3a, there are many features at the core of the outer zone ($3 \lesssim L \lesssim 4.5$) that are not well discerned in the partial outer belt view afforded in Figure 3b.

The complete view of the radiation belt particle populations is revealed in Figure 3c. This shows the full sweep of electron measurements from REPT for $1 \lesssim L \lesssim 7$ over the 6-year run of RBSP data. The inward radial extent of many electron enhancements, the full nature of loss episodes, the evolution of inward radial diffusion events, and the general richness of electron flux variability throughout the LEO-to-MEO realm are amply demonstrated by having the complete picture provided by the continuous Van Allen Probes data.

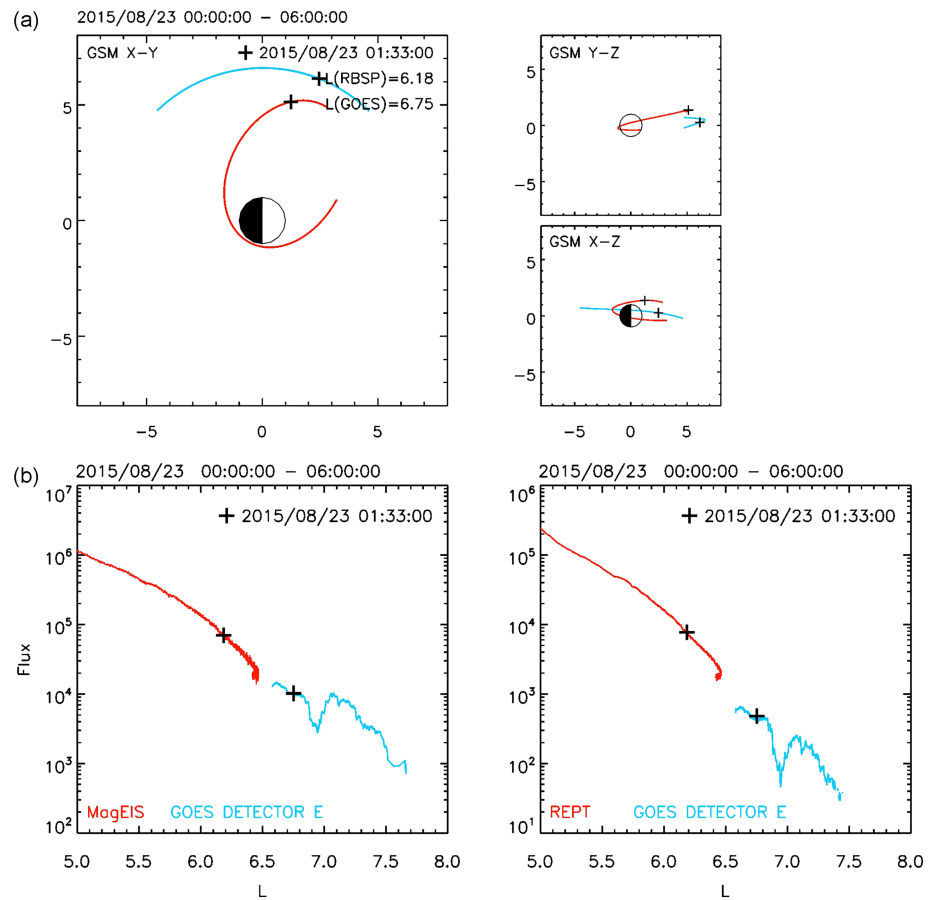


Figure 7. Similar to Figure 5 but for the period 0000–0600 UT on 23 August 2015.

In light of the results shown in Figure 3, we have sought to compare and contrast the data regularly gathered by GOES sensors with the more complete information obtained from the Van Allen Probes. To do more statistical comparisons, we have chosen to assemble daily averaged fluxes from GOES-15 sensors and also daily averaged measurements of various sorts from Van Allen Probes sensors. In this analysis we have focused on two standard integral flux channels from GOES-15, viz, the $E > 0.8$ MeV channel and the $E > 2$ MeV energy channel. As shown below, we have initially used simple daily averages of GOES data to get started. However, we have subsequently used more selective averages—for reasons that will be clear—and have therefore used L sorting methods. For both Van Allen Probes data and for GOES-15 data we have used McIlwain L values calculated in the T89 model framework (Tsyganenko, 1989).

2.1. Initial Statistical Comparisons

Some earlier studies (e.g., Onsager et al., 2004) have compared simultaneous measurements from multiple GOES spacecraft. In so doing, this kind of earlier work has shown evidence of magnetic latitudinal dependences indicative of substantial radial flux gradients. With the availability of Van Allen Probes data, it is possible to have much more extensive examination of radial flux properties near GEO. Our initial expectation in this study was that comparing daily averages of GOES-15 fluxes (assumed nominally to be at $L \sim 6.6$) with Van Allen Probes data at a fixed L (initially taken as $L = 6.0$) would produce rather close correlation and essential flux agreement. This often was not the case.

Figure 4 shows our initial comparison results. In Figure 4a, we plot the daily flux value for $E > 0.8$ MeV electrons at $L = 6.0 (\pm 0.05)$ against the corresponding daily average flux for GOES-15. Rather than seeing a one-to-one correspondence, we have found that the Van Allen Probes fluxes (actually for the MagEIS energy interval $E = 0.8$ –4 MeV) were almost always larger than the GOES integral flux by a substantial factor. As shown by the blue and red diagonal lines, the Van Allen Probes fluxes were most commonly a factor of 5

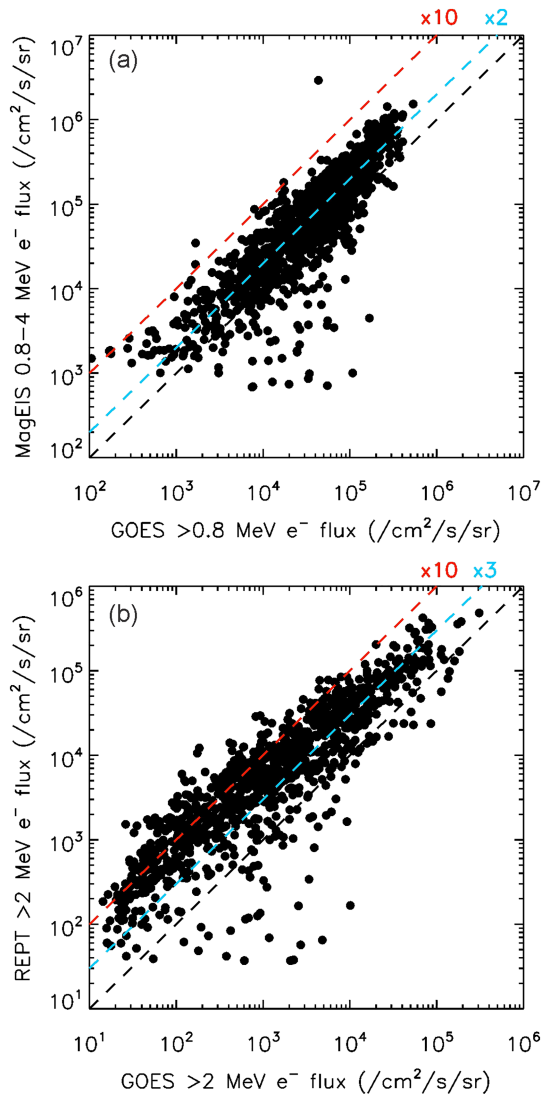


Figure 8. Scatterplots of daily flux averages from the Van Allen Probes versus the GOES-15 “E” when both spacecraft were at $L = 6.6 \pm 0.05$. (a) Daily values of $E > 0.8$ MeV electrons from Van Allen Probes A versus comparable GOES-15 measurements. (b) Similar to (a) but for electrons with energies $E > 2$ MeV. Data from 1 September 2012 to 1 September 2018 are included in the plots.

are for RBSP measurements across L values from $L \sim 5.0$ to $L \sim 6.0$. On the other hand, the fluxes from $L \sim 6.5$ to $L \sim 7.8$ measured by GOES-15 sensors fall off very strongly with increasing L. This is particularly evident for the $E > 2$ MeV measurements. In the various panels, black crosses mark the point in time at which the two spacecraft were at closest geographic approach (0739 UT). At that time, the T89 magnetic field model suggests that the spacecraft were ~ 1.3 L units apart. Figure 5b shows at that instant the $E > 0.8$ MeV flux value at RBSP-A was $\sim 4 \times 10^5$ ($\text{cm}^2 \text{ s sr})^{-1}$, while at GOES-15 the flux level was only $\sim 7 \times 10^4$ ($\text{cm}^2 \text{ s sr})^{-1}$. This suggests a factor of nearly six flux disparity across about one Earth radius (~ 1.3 L units). Even more notably, the $E > 2$ MeV flux at 0739 UT for RBSP-A was $\sim 3 \times 10^4$ ($\text{cm}^2 \text{ s sr})^{-1}$, while for GOES the flux was only $\sim 2 \times 10^3$ ($\text{cm}^2 \text{ s sr})^{-1}$ —a ratio of 15. These results show quite obviously that even under rather quiet (nonstorm) conditions, the GEO satellites can effectively be on much higher than nominal ($L \sim 6.6$) field lines. Moreover, the radial gradient of electron fluxes, especially at high electron energies are, and often can be, quite strong outward of $L \sim 6.0$.

greater than the GOES fluxes measured on the same day. In many cases, the Van Allen Probes values were a factor of 10 higher than GOES (and sometimes even a factor of 20 higher).

The differences between Van Allen Probes and GOES were found to be even larger at higher energies. Figure 4b shows daily averaged integral measurements above 2 MeV at $L = 6.0$ from the REPT sensors on Van Allen Probes plotted versus the corresponding daily average $E > 2$ MeV fluxes from GOES-15. The Van Allen Probes flux values were seen to be typically a factor of more than 10 larger than GOES and occasionally exceeded a factor of 100 higher than the GOES values. Such large flux differences between $L = 6.0$ and a nominal location of $L = 6.6$ clearly deserved closer inspection.

2.2. Detailed Flux Comparisons

In order to understand in more detail why GOES and RBSP daily flux values differed so greatly for measurements seemingly in such similar parts of the outer Van Allen zone, we have examined dozens of cases where GOES-15 was physically close to one of the Van Allen Probes spacecraft. We generally sought cases where the two spacecraft were not only close in radial distance from Earth but also proximate in all three GSM (Geocentric Solar Magnetospheric) coordinate senses (X - Y , Y - Z , and X - Z). In this section, we present several illustrative examples of such local flux comparisons.

Figure 5 shows positional information and flux comparisons for a non-storm time interval from 0300 UT to 1100 UT on 7 January 2017. The upper portion of the figure (panels in part (a)) show projections of the GOES-15 orbit (in blue) for that entire time interval in various GSM planes. The closest approach of GOES with Van Allen Probes A (orbit shown in red) occurred at 0739 UT on 7 January. At that time, the two spacecraft were less than $1 R_E$ apart in any rectilinear dimension and they were especially close together in the Z_{GSM} sense. The orbits of GOES and the RBSP-A spacecraft swept out broad swaths in the premidnight and midnight sectors of the magnetosphere during the 8-hour interval under examination.

Figures 5b and 5c, respectively, show temporal comparisons for $E > 0.8$ MeV and $E > 2$ MeV fluxes for the entire period 0300–1100 UT. The data from the two spacecraft are presented as integral flux values (electrons/ cm^2 -s-sr) versus L value. As noted above, the L values are computed here (and throughout this study) using the T89 model. What is striking in Figure 5b—and even more so in Figure 5c—is how flat the flux values

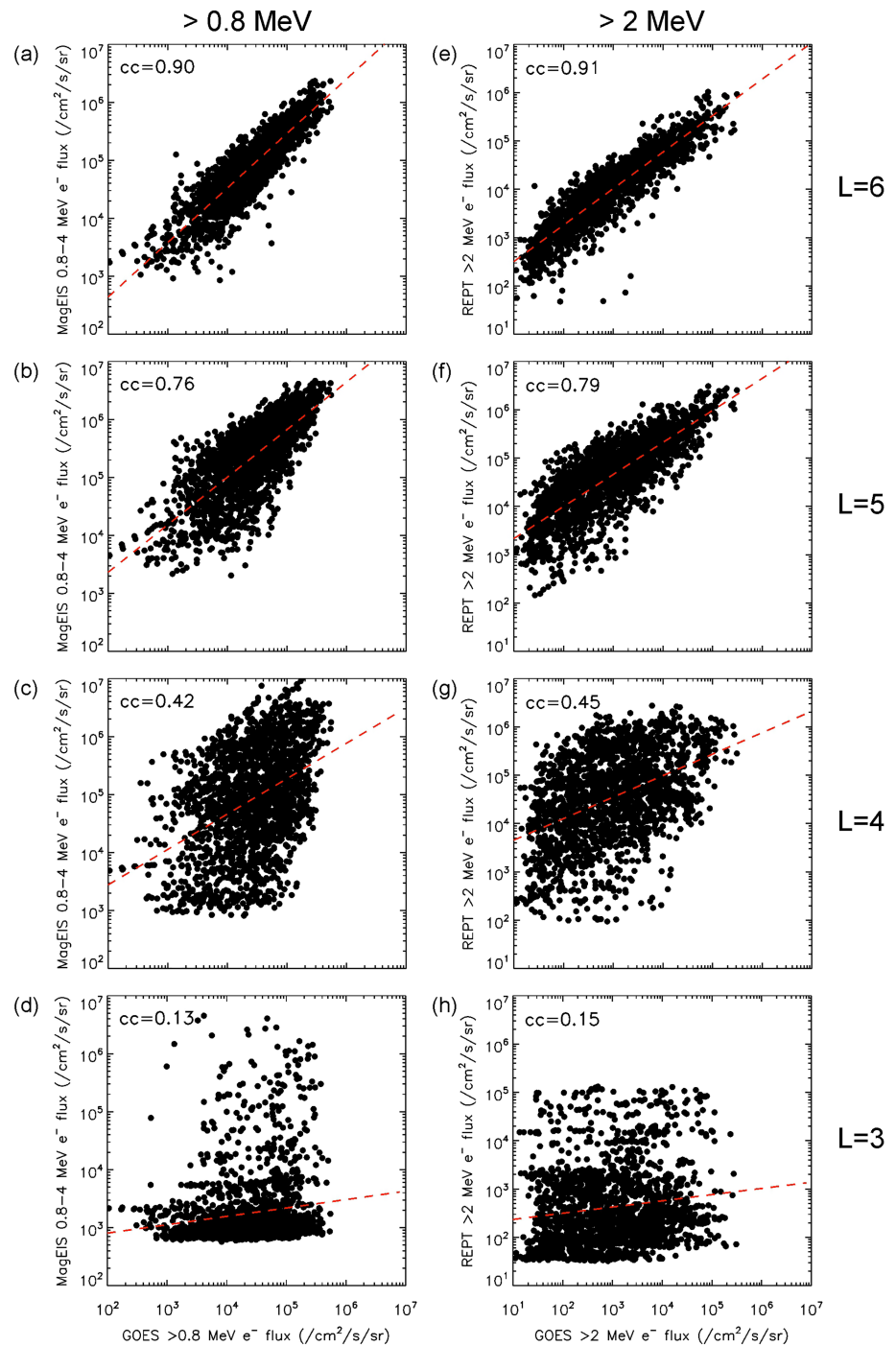


Figure 9. Statistical scatterplots similar to Figure 8 but for different L ranges of the Van Allen Probes measurements. (a–d) $E > 0.8$ MeV data, while (e–h) $E > 2$ MeV results. The rows from top to bottom correspond, respectively, to Van Allen Probes being at $L = 6.0 \pm 0.05$, $L = 5.0 \pm 0.05$, $L = 4.0 \pm 0.05$, and $L = 3.0 \pm 0.05$.

Another example of flux comparison between GOES and RBSP sensors is shown in Figure 6. The format of the figure is exactly the same as for Figure 5. In this case, we examine flux profiles when GOES-15 and RBSP-A were generally on the dayside of Earth (see Figure 6a) and reached closest approach to one another at ~ 2030 UT on 23 December 2015. As in the example of 7 January 2017, GOES and RBSP were about $1R_E$ apart in radial distance at closest approach and were at nearly identical Z_{GSM} locations. This interval of time

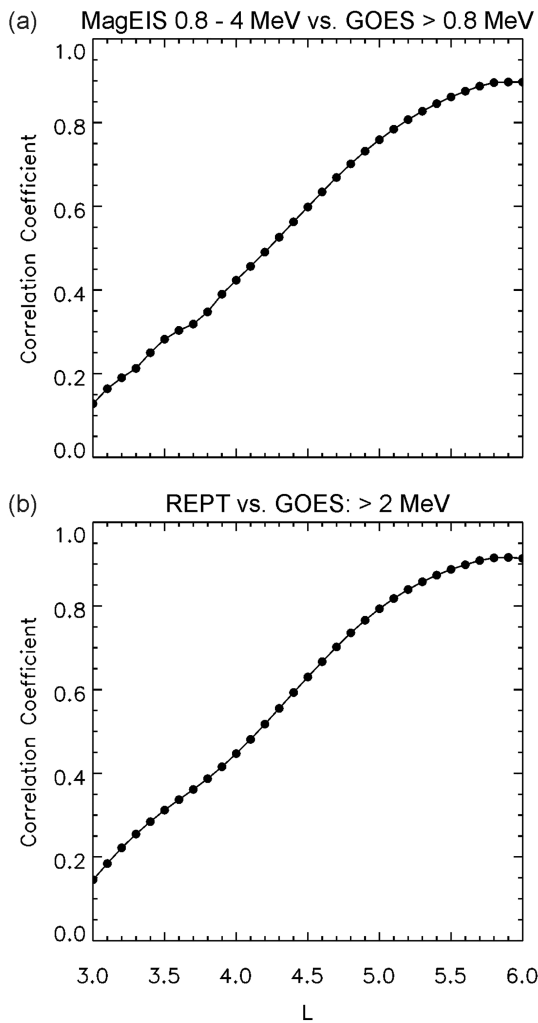


Figure 10. (a) Correlation coefficients between the log of $E > 0.8$ MeV electron fluxes measured at various L values by Van Allen Probes and the log of such electrons measured by GOES-15 at $L = 6.6 \pm 0.05$ over a period September 2012 to August 2018. (b) Similar to (a) but for electrons with $E > 2$ MeV.

corresponded to the recovery phase of a relatively intense geomagnetic storm (the storm time geomagnetic index reached a peak value of $Dst \sim -155$ nT at 2300 UT on 20 December 2015).

For this still-active geomagnetic period following the storm main phase, Figures 6b and 6c demonstrate that the fluxes measured by MagEIS and REPT, respectively, on board the RBSP-A spacecraft showed a quite substantial flux gradient from $L = 5.0$ to $L \sim 5.7$ over the time period 1600 UT to 2400 UT on 23 December. GOES-15 data showed a similar radial gradient trend, but under the active geomagnetic conditions and on the day-side of the magnetosphere, GOES 15 only moved across an L -range of $6.4 \lesssim L \lesssim 6.7$ during its entire dayside passage. At the time of closest approach (2030 UT) the >0.8 MeV fluxes were $\sim 3 \times 10^5$ (RBSP-A at $L \sim 5.7$) and $\sim 1.2 \times 10^5$ (GOES-15 at $L \sim 6.4$). This implies a radial gradient of only a factor of 2–3 over a $1-R_E$ span. For $E > 2$ MeV electrons shown in Figure 6c, the gradients were obviously even stronger. At 2030, RBSP-A measured $\sim 4 \times 10^4$ $(\text{cm}^2 \text{ s sr})^{-1}$, while GOES-15 measured $\sim 8 \times 10^3$ $(\text{cm}^2 \text{ s sr})^{-1}$ for a ratio of about 5 over the $1-R_E$ separation. As for the previous example in Figure 5 the data in Figure 6 show how satisfactorily the flux values between RBSP and GOES appear to agree with one another (if the data trends are extended upward and downward in L between the two spacecraft).

A final example of detailed comparison shown here in Figure 7 is for a small ($Dst \sim -43$ nT) geomagnetic storm on 23 August 2015. As shown in Figure 7a, the two spacecraft were in relatively close conjunction toward the dusk sector, but were generally a bit further apart in GSM X , Y , and Z senses than the prior examples. Over the period 0000 UT to 0600 UT, RBSP-A covered the L range up to $L \sim 6.4$, while GOES-15 traversed the range $6.6 \lesssim L \lesssim 7.7$. At the closest physical separation, RBSP-A was at about $L = 6.2$ and GOES-15 was at about $L = 6.7$. Even at such close L separations, the $E > 0.8$ MeV electron fluxes differed by nearly a factor of 8, while the $E > 2$ MeV electrons showed a factor of $\gtrsim 20$ higher flux at RBSP compared to GOES.

Thus, large radial gradients under a variety of geomagnetic conditions explain rather convincingly why the simple daily-average flux comparisons in Figure 4 showed such obvious large disagreements between RBSP and GOES sensors.

2.3. Refined Statistical Comparisons

In light of observations such as those shown in the last section, it is clear that during any one day GOES generally samples quite a different range of L values than does an RBSP spacecraft. Consequently, to make truly meaningful absolute comparisons, it is necessary to select more deliberately those periods when both GOES and RBSP spacecraft were on essentially the same L shells. Because of varying geomagnetic activity (and resulting magnetic field distortions), not every day has such L shell overlap, but portions of many days do have both GOES and RBSP on the nominal GEO L shell of 6.6. We have selected times when the T89 model indicates such common L range sampling and those results (to be compared with Figure 4 above) are shown here in Figure 8.

As evident in Figure 8a, choosing averages for those days when both the MagEIS sampling (on RBSP) and the GOES-15 sensor sampling were restricted to $L = 6.6 \pm 0.05$ improves the correlation immensely compared to the results of Figure 4a. With the selected data averaging, the RBSP electron fluxes with $E > 0.8$ MeV often fall very near the GOES-15 counterparts and the general agreement is such that RBSP flux values were typically about a factor of 2 higher than the GOES values (see blue diagonal line in Figure 8a). Virtually all the RBSP points lie within a factor of ~ 5 of the corresponding GOES daily value in the figure across the entire range from low to high flux values.

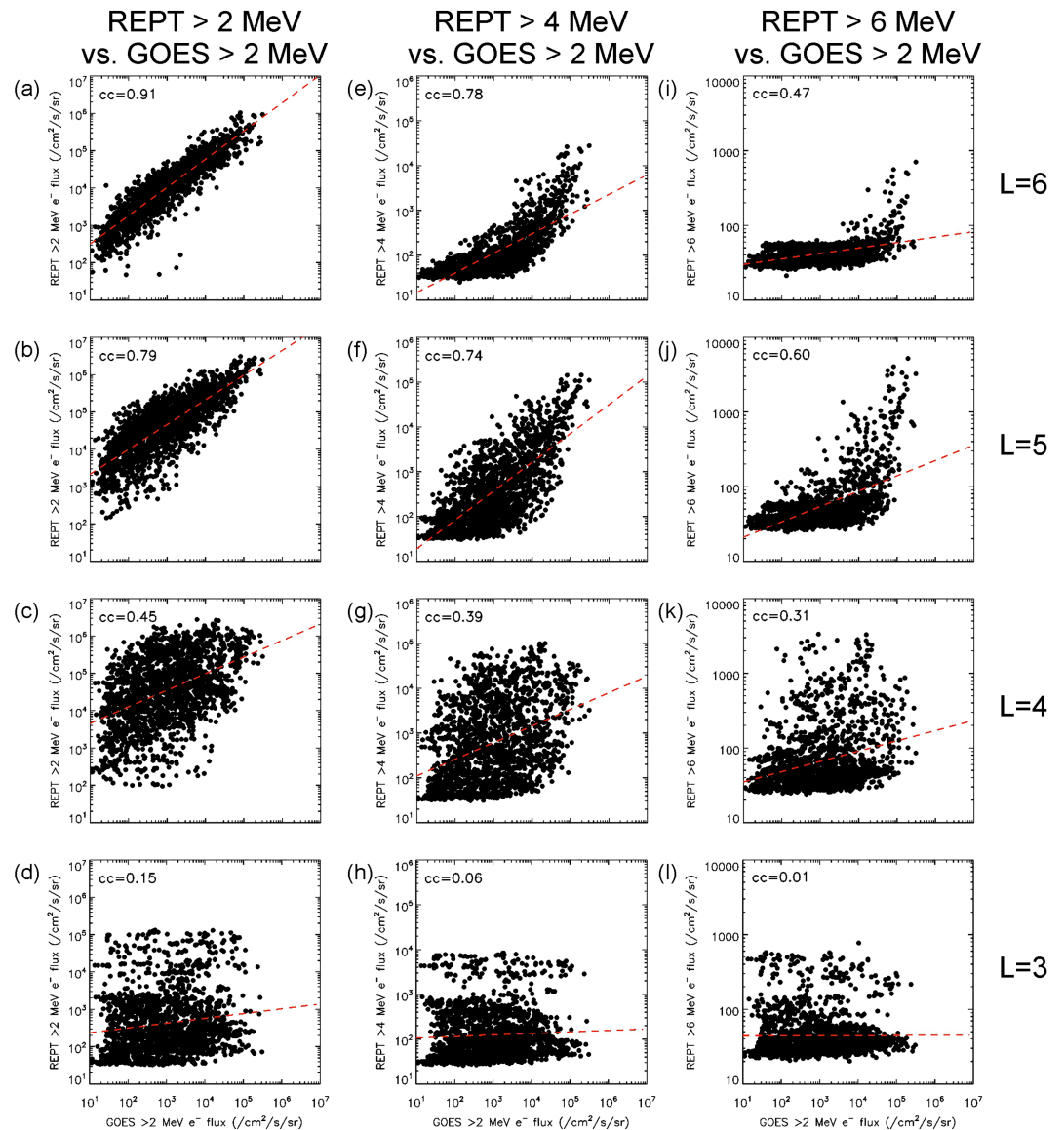


Figure 11. Scatterplots similar to Figure 9 but for a range of threshold energies of the Van Allen Probes sensors. (a–d) A repeat of Figures 9e–9h. (e–h) For Van Allen Probes electrons with $E > 4$ MeV. (i–l) For Van Allen Probes electrons with $E > 6$ MeV.

The agreement for the $E > 2$ MeV fluxes is not as good between GOES and RBSP for $L = 6.6$. This comparison of available data is shown here in Figure 8b. The figure demonstrates that the vast majority of RBSP daily-average flux values fall within a factor of ~ 10 of the corresponding GOES flux values (see red diagonal line Figure 8b). At the highest flux levels (i.e., most active times), the agreement appears better (factor of ~ 3 separation). But at the lowest flux values, the RBSP data appear to be systematically higher than the GOES counterparts by a factor of ~ 10 . Such differences notwithstanding, the RBSP-GOES agreement seen in Figure 8b is immensely better than that without deliberate L selections (as in Figure 4b): Possible reasons for the activity-dependent disagreement between GOES and RBSP averages in Figure 8b will be discussed later in this paper.

2.4. More Widely Separated L Comparisons

Because of the wide range of radial distances (and L values) sampled by the Van Allen Probes during each orbit, we can examine how radiation belt fluxes away from GEO altitudes compare with the baseline

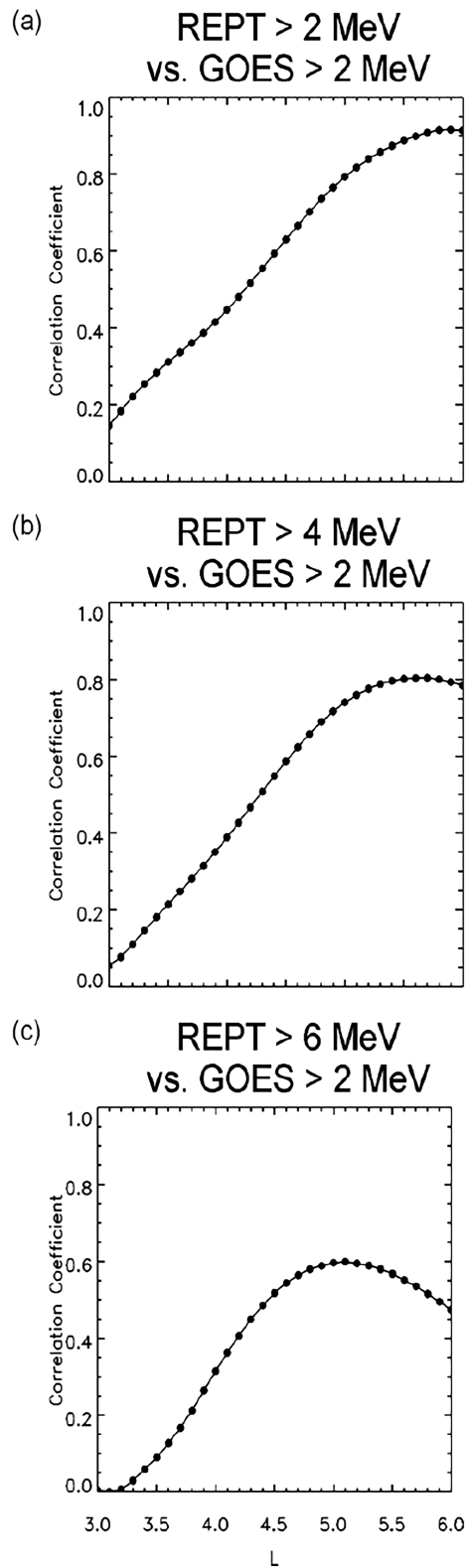


Figure 12. Similar to Figure 10b showing correlation coefficients versus L for Van Allen Probes versus GOES-15 electrons with $E > 2$ MeV. (a) Van Allen Probes electrons with $E > 2$ MeV. (b) Van Allen Probes electrons with $E > 4.0$ MeV. (c) Van Allen Probes electrons with $E > 6.0$ MeV.

GOES measurements. In this kind of comparison, we take as reference data the daily average GOES-15 fluxes at $L = 6.6 \pm 0.05$. We then sort and compute the daily average values of >0.8 MeV and >2 MeV fluxes for a selected set of sampled L values from the RBSP spacecraft. These kinds of results are shown here in Figure 9.

Looking first at $L = 6 (\pm 0.05)$ flux values from RBSP compared to GOES $L = 6.6 (\pm 0.05)$ flux values, Figures 9a and 9e show the >0.8 MeV and >2 MeV results, respectively. For $E > 0.8$ MeV data, we see that the correlation analysis for the log-log flux comparison yields a correction coefficient (c.c.) = 0.90. The best, least squares fit through the scatter of points shows the RBSP fluxes at $L=6.0$ to be about 4 times the corresponding GOES-15 values. On the other hand, the RBSP logarithmic flux values in Figure 9e are not as linearly related to GOES at >2 MeV as they are for $E > 0.8$ MeV. The REPT-to-GOES correlation coefficient is high (c.c. = 0.91) in Figure 9e, but at the low activity level end, the REPT fluxes were 200–300 times higher than at GOES-15. This separation reduces to virtually no statistical difference between the two spacecraft at higher flux levels ($\gtrsim 10^5 (\text{cm}^2 \text{ s sr})^{-1}$).

At L values lower than $L = 6.0$, the correlation coefficients diminish progressively between the flux values at RBSP and the baseline values at GOES. Also, as would be expected in the heart of the outer radiation zone ($L = 4-5$), the average electron fluxes measured by RBSP sensors are substantially larger for each daily average as compared to GOES at $L = 6.6$. For RBSP at $L = 5.0 (\pm 0.05)$, the >0.8 MeV correlation coefficient is found to be c.c. = 0.76 (Figure 9b), while for $E > 2$ MeV, the value is c.c. = 0.79 (Figure 9f). Comparing $L = 4.0$ fluxes with $L = 6.6$ fluxes yields c.c. = 0.42 for $E > 0.8$ MeV (Figure 9c) and c.c. = 0.45 for $E > 2$ MeV (Figure 9g). Dropping even lower toward the inner edge of the outer zone at $L = 3.0 (\pm 0.05)$ in Figures 9d and 9h, the correlations are generally approaching insignificance (c.c. $\sim 0.13-0.15$).

From these results, we conclude that there can be reasonable statistical confidence in using baseline ($L = 6.6$) GEO measurements to estimate energetic electron populations in the radiation belts to around $L = 5$. However, by $L = 4.0$ the correlations with $L = 6.6$ are marginal and even deeper in the magnetosphere ($L \lesssim 4.0$) there is little relationship between daily electron flux values at GEO and those flux values experienced by a MEO spacecraft.

Figure 10 shows the correlation coefficients calculated between RBSP-measured fluxes at every 0.1 unit of L as compared to the baseline GOES-15 measurements at $L = 6.6$. Obviously, the correlations break down progressively as the RBSP measurements are made further and further away from the GEO belt. Both the >0.8 MeV (Figure 10a) and the >2 MeV (Figure 10b) correlations peak out just above c.c. values of $r = 0.9$, meaning that about 80% (r^2) of the variance of RBSP-measured fluxes can be related to the measurement of GOES.

2.5. Energy Dependences

The REPT instruments on board the Van Allen Probes generally make high-quality measurements across all L values in the electron energy range $1.5 \lesssim E \lesssim 10$ MeV (Baker et al., 2012, 2019). Thus, we can examine the dependences of GOES-15 correlations not only with L value but also with increasing RBSP electron energy. For such studies we again take as a baseline the GOES-15 ($E > 2$ MeV) measurements at $L = 6.6$. Figure 11 then shows such scatterplots for REPT $E > 2$ MeV (Figures 11a–11d), for REPT $E > 4$ MeV (Figures 11e–11h), and for REPT $E > 6$ MeV (Figures 11i–11l). The horizontal rows correspond (top to bottom) to $L = 6$, $L = 5$, $L = 4$, and $L = 3$.

The scatterplots in Figures 11a–11d are essentially repetitions of material shown also in Figures 9e–9h. On the other hand, the $E > 4$ MeV and $E > 6$ MeV correlations show several interesting new features. Among these are that the $E > 4$ MeV behavior is closely analogous in a statistical sense to the $E > 2$ MeV behavior (see Figures 11e–11h). On the other hand, the “ultrarelativistic” electrons (cf. Baker et al., 2019) with $E > 6$ MeV show quite different behavior than the 2 MeV electrons at $L = 6.6$. We conclude that at very high energies ($E \gtrsim 5$ MeV) and relatively low L values ($L \lesssim 4.0$), the GOES measurements give only a very limited indication of what might be happening in the radiation belts on any given day.

The overall correlation coefficients calculated for various L values and at several RBSP energy levels are shown in Figure 12. As noted, the $E > 4$ MeV behavior is found to be quite analogous in most respects to that for the RBSP $E > 2$ MeV energy range. On the other hand, the correlation between GOES >2 MeV electrons

and RBSP >6 MeV electrons peaks at $L \sim 5.0$ (Figure 12c) and diminishes substantially both above and below this L value. This is very different from the 2–4 MeV behavior.

3. Discussion and Conclusions

As noted in section 1, it has been a common practice to use the long, continuous runs of GEO operational data to perform various kinds of statistical analyses, often looking at energetic electron flux dependences on solar wind forcing parameters, for example. In many instances, GOES or other GEO data have also been used as a monitor of radiation belt properties in order to ascribe (or refute) space weather as a cause of spacecraft operational anomalies. As we have shown in this study, GOES energetic electron data near $L = 6.6$ correlate relatively highly with measured fluxes from the Van Allen Probes when the latter spacecraft were in the range $4.5 \lesssim L \lesssim 6$.

On a more positive note, we found in this study that the flux values measured by GOES-15 sensors matched up very well with Van Allen Probes sensors when the spacecraft were physically close to one another. This suggests that the absolute accuracy (or at least the cross-calibration) of the operational sensors with the scientific sensors is good. Especially at the energy of $E > 0.8$ MeV, the statistical relationships of the daily average fluxes at $L = 6.6$ was reasonable across all flux levels from low to high (see Figure 8a).

Such close correspondence was not found for all the $E > 2$ MeV measurements (see Figure 8b). At the highest GOES flux levels ($\gtrsim 10^4$ (cm² s sr⁻¹)) the Van Allen Probes data agreed with GOES-15 to within a factor of about 3 for $L = 6.6$. But at lower activity levels, the $E > 2$ MeV electron fluxes for Van Allen Probes were more typically a factor of ~ 10 higher than GOES-15 (Figure 8b). We reasonably can ask whether this is a calibration issue with one (or both) of the GOES/RBSP sensor systems or whether there might be a geophysical explanation for fluxes to be so different at lower activity levels.

In Appendix A, we examine some aspects of the Van Allen Probes higher-energy electron measurements (both flux behavior and pitch angle responses) as compared with GOES-15. We also consider orbital properties of the Van Allen Probes vehicles. At this point we have no reason to suspect systematic errors in either the GOES or the Van Allen Probes (REPT) data sets. Rather, we find that orbital, pitch angle, and radial gradient effects explain essentially all observed statistical relationships presented in this study.

As shown in Appendix A, a cross comparison of the REPT and MagEIS sensor data for electron measurements at energies $E=2-4$ MeV show very good agreement (to within a factor of 2). Detailed comparisons between RBSP and GOES for specific events (Figures 5–7 and in Appendix A) also suggest very good cross calibration of the operational sensors with the Van Allen Probes science measurements. However, as also shown in Appendix A, the fact that GOES sensors integrate over a pitch angle range in a fixed staring direction could account for GOES fluxes often being low in daily averages compared to the complete pitch angle measurements by RBSP sensors. This is due to frequent “butterfly” pitch angle distributions at high L regions mostly at night side.

The differences seen between Van Allen Probes daily average fluxes and ostensibly similar GOES-15 daily averages can, we believe, be dominantly explained by the strong radial gradients that occur for electron fluxes, especially at relatively high energies ($E > 2$ MeV) and during quieter geomagnetic conditions. As shown here—especially in Figure 5—during relatively quiet times the flux of electrons is pretty flat from $L \sim 5.0$ out to $L \sim 6.0$. However, beyond that radial distance, the fluxes drop precipitously, especially for the $E > 2$ MeV electrons. Thus, for daily averages of GOES data—either the simple averages in Figure 4 or the most refined averages near $L = 6.6$ in Figures 8, 9, or 11—the GOES fluxes will be relatively low due to sampling high L values. On the other hand, the Van Allen Probes data acquired at $L = 6.0$ (or $L = 5.0$, $L = 4.0$, etc.) will be rather high owing to the flat radial gradient inside GEO. Only during quite disturbed conditions with high electron flux values (when the gradient beyond $L = 6.6$ flattens out further) would the GOES, and RBSP daily flux averages agree closely with one another.

In summary, we have used concurrent GOES and Van Allen Probes data to illuminate the issue of when and where operational GEO data can be used to monitor energetic electron radiation belt properties away from the geostationary orbit proper. These results demonstrate that for many MEO (and LEO) locations, one must exercise considerable care in using GEO monitoring data to understand local radiation belt properties and flux levels. Quite obviously, there is no substitute for measuring energetic electron flux levels directly at

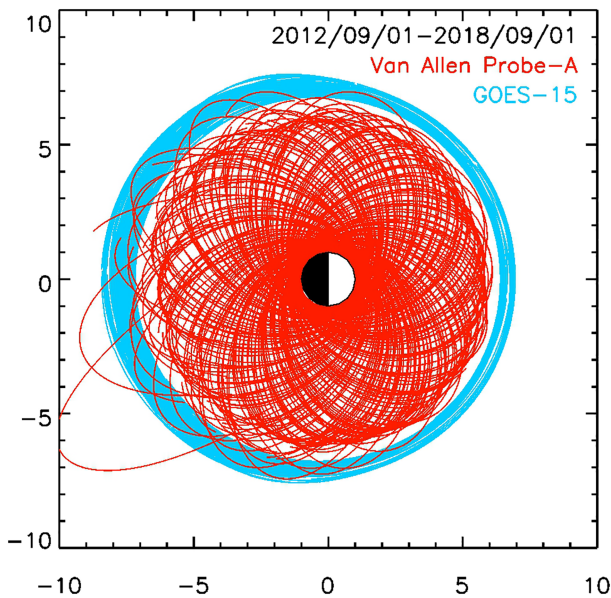


Figure A1. L versus MLT (magnetic local time) plot for orbits of Van Allen Probe A (in red) and GOES (in blue) from September 2012 to August 2018. One orbit per 10 days is shown.

low L values ($L \lesssim 4.0$) rather than relying solely on surrogate measurements at higher altitude locations. We rue the day that Van Allen Probes data no longer will be available.

Appendix A: Supplementary Information

The main studies presented in this paper raise questions about some puzzling statistical relationships that emerge looking at daily averages of GOES and Van Allen Probes data. It is important to examine carefully the orbital characteristics of the two spacecraft and to think in detail about what averaging procedures may really imply about flux comparisons.

In Figure 2 above, we presented a schematic diagram of the orbits of the GOES and Van Allen Probes spacecraft in terms of simple geocentric radial distances. However, the actual particle properties going into our statistical comparisons in this paper are more appropriately considered in terms of L values. In the main text of this paper, we have noted that throughout our study, we have used the T89 model to compute L values. In Figure A1, we show (in blue) the orbits of GOES 15 (in terms of L values) for the period 1 September 2012 to 1 September 2018. To reduce clutter, we show orbits for only every tenth day. In the red traces, we show the corresponding orbits for the Van Allen Probes A spacecraft for the same 6-year period.

Figure A1 shows that GOES-15 orbits for the entire period of our study were tightly bounded between $L \simeq 6.0$ and $L \simeq 7.0$ near the local noon sector. The modeled results also show that the Van Allen Probes orbits with apogee near local noon were never seen to extend much beyond $L \simeq 6.0$ during the 6-year period of this study. Thus, on the dayside magnetosphere we never would have had Van Allen Probes samples at $L = 6.6$ to compare directly with concurrent GOES samples at $L = 6.6$.

Along the flanks of the magnetosphere and on the night side, there were many more instances where GOES and Van Allen Probes orbits overlapped in L values. These were times when the magnetosphere had magnetic field lines more “stretched” due to strong solar wind interactions. On the nightside of the magnetosphere, the GOES-15 orbital “band” was generally much broader than on the dayside, and in some extreme cases the T89 model suggested that the RBSP-A spacecraft was on very distended field lines.

These orbital results emphasize that we must be cautious in interpreting statistical scatterplots where we have selected both GOES and RBSP to be on the nominal $L = 6.6$ magnetic shell. While this could be reasonable for RBSP apogee periods on the nightside, almost no RBSP daily data samples would be included from the times that the RBSP spacecraft apogee was on the dayside.

We have the ability to check independently on the general validity of the RBSP high-energy electron flux values. The MagEIS instrument (Blake et al., 2013) measures up to 4 MeV in energy. Thus, we can form an “integral” channel for MagEIS from 2 to 4 MeV that can be directly compared with the more complete integral measurements ($E > 2$ MeV) from the REPT sensor system (Baker et al., 2012). Figure A2 shows the several detailed events examined in this paper (see Figures 5–7 above) where now we have included the MagEIS $E = 2$ –4 MeV flux profiles versus L, along with the REPT ($E > 2$ MeV) and GOES-15 ($E > 2$ MeV) flux profiles previously shown. We see from all three event periods in Figures A2a–A2c that the MagEIS data parallel the REPT data almost perfectly. The principal difference is that the MagEIS fluxes run lower—typically by a factor of 2 or 3—due to MagEIS not including the energetic electron fluxes with $E > 4.0$ MeV. We take these results as good validation and verification of the overall Van Allen Probe high-energy electron measurement set.

In Figure A3 we make some further statistical comparisons of data between GOES-15 electron measurements ($E > 2$ MeV) over all L values with RBSP-A data sets taken at $L = 6.0$. Figure A3a is similar to Figure 4b showing daily averages for the $E > 2$ MeV REPT data at $L = 6.0$ (± 0.05) compared to the $E > 2$ MeV GOES-15 data over all L values. Figure A3b shows the corresponding plot of $\text{MeV} \leq E \leq 4$ MeV electron fluxes versus the GOES $L = 6.6$ baseline data. There is wide scatter in both panels (a) and (b), but the correlations are

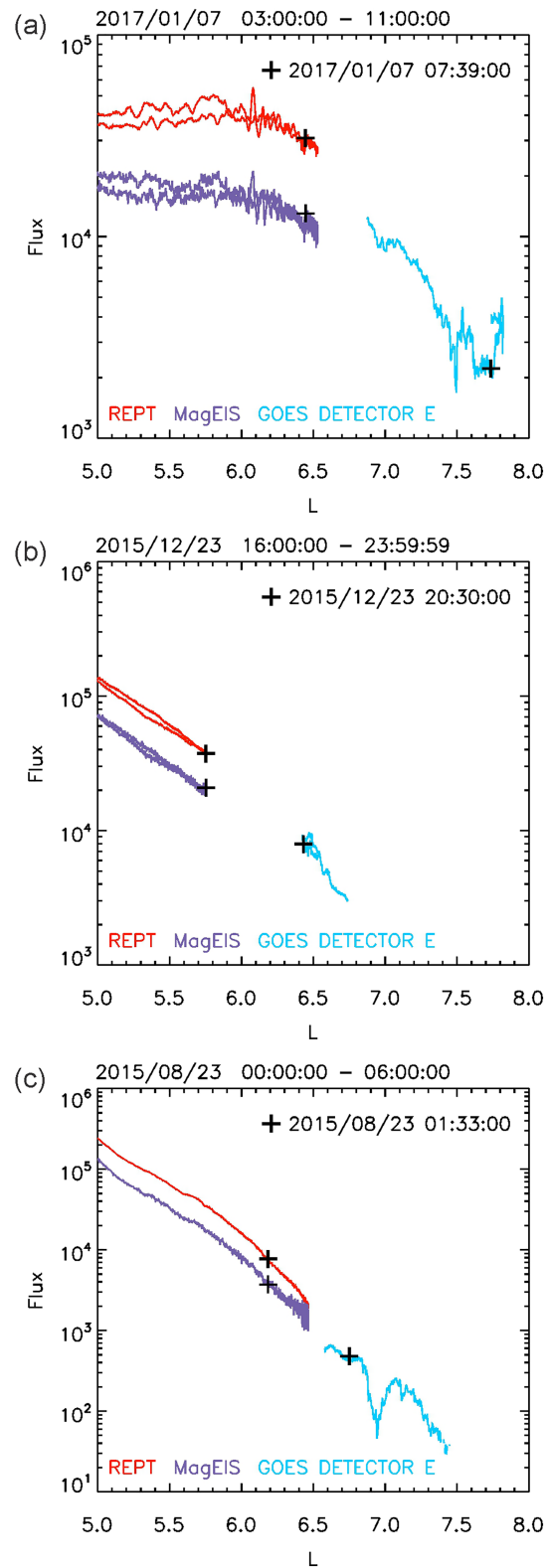


Figure A2. Comparison of REPT >2 MeV, MagEIS 2–4 MeV, and GOES >2 MeV electron fluxes during (a) 0300–1100 UT on 7 January 2017, (b) 1600–2359 on 23 December 2015, and (c) 0000–0600 UT on 23 August 2015. (Note that the scales of the y axes are different for these panels.)

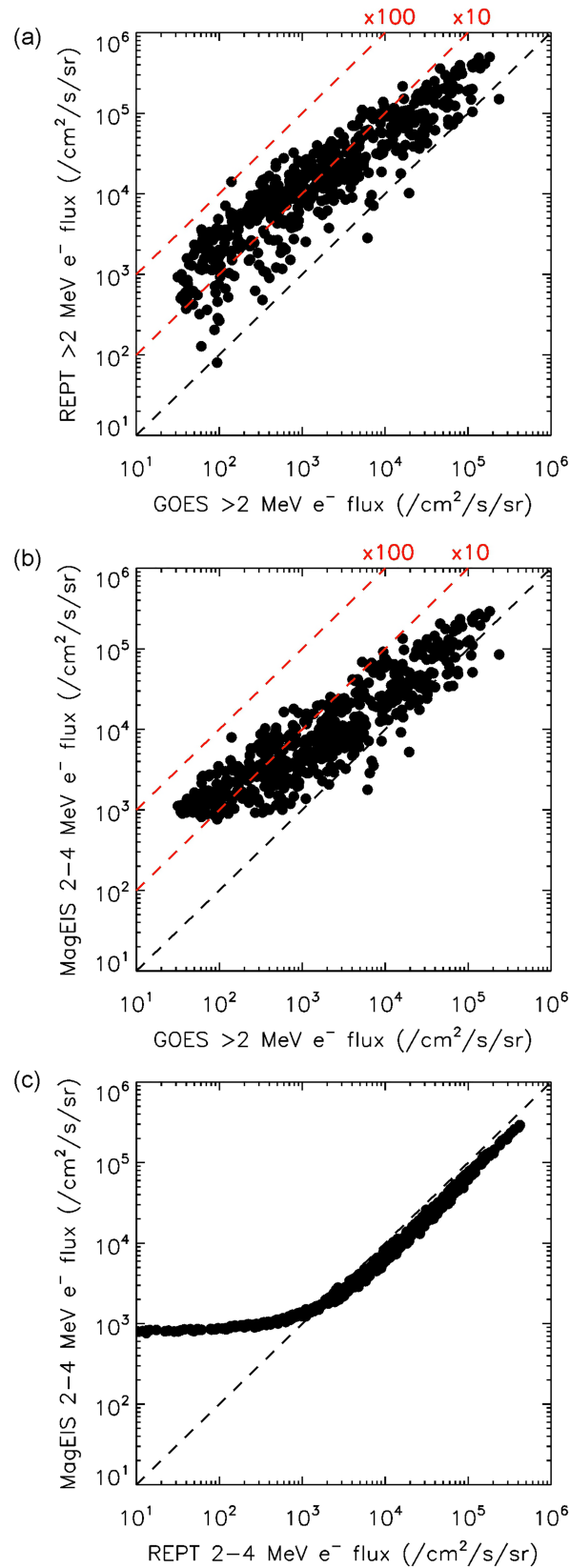


Figure A3. Scatter plots of (a) REPT $E > 2$ MeV and (b) MagEIS 2–4 MeV electron daily averaged fluxes at $L = 6$ versus GOES >2 MeV electron daily averaged fluxes at $L = 6.6$ using data from 1 January 2017 to 1 September 2018. (c) Scatterplot of MagEIS versus REPT data in the energy range 2–4 MeV for same period.

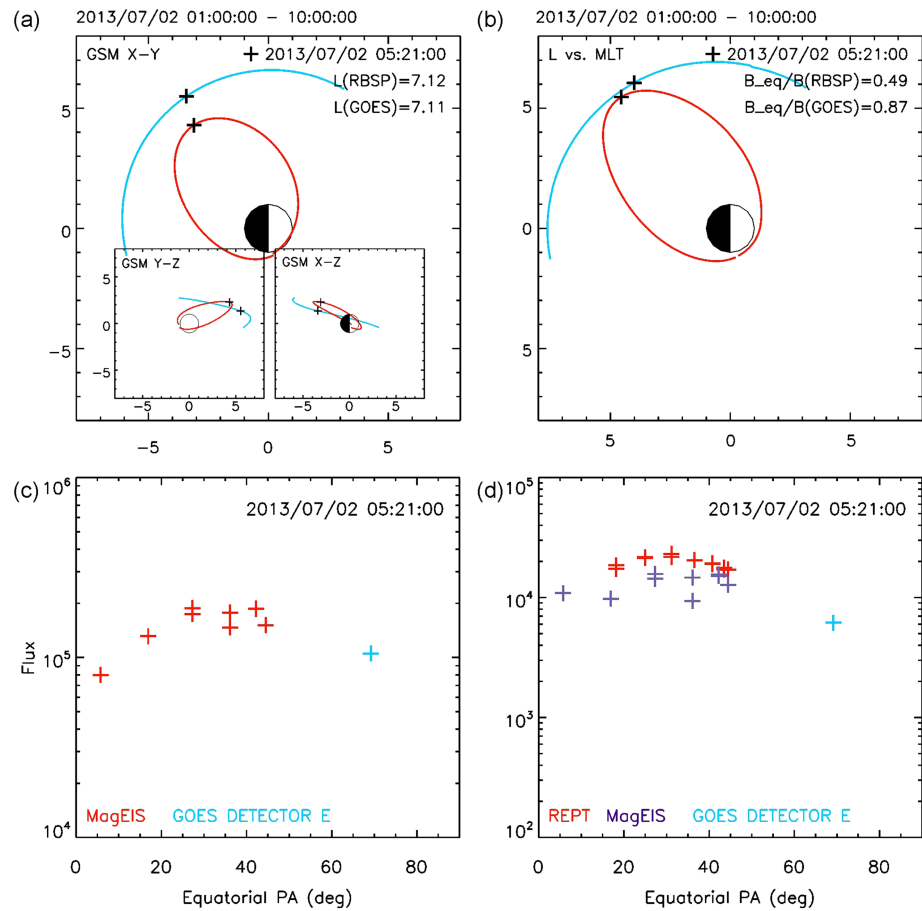


Figure A4. (a, b) Orbit information in GSM plane and in L versus MLT and (c, d) pitch angle resolved flux comparison of Van Allen Probe A and GOES-15 at 0521 UT on 2 July 2013. (assuming GOES-15 measures locally mirroring particles).

strong. In Figure A3c, we plot the scatter diagram of MagEIS 2–4 MeV fluxes (at $L = 6.0$) against the REPT 2–4 MeV fluxes (also at $L = 6.0$). We see that above flux levels of $\sim 10^3$ ($\text{cm}^2 \text{ s sr}^{-1}$), the REPT and MagEIS data correlate almost perfectly. Clearly at lower activity (flux) levels for REPT, the MagEIS data reach background levels and the linear correlation breaks down.

A final point to bear in mind is that GOES-15 is a three-axis stabilized spacecraft and so the sensors stare in a fixed orientation. In this paper we have used the EPEAD “E” sensor for determining the GOES flux values. On the other hand, the RBSP spacecraft are spinning spacecraft. Typically, GOES would be integrating over a wide range ($\sim 50^\circ$ – 150°) of electron local pitch angles with a response function peaked around local 100° pitch angle, while Van Allen Probes (both MagEIS and REPT) would sample nearly all local electron pitch angles.

In Figure A4, we show an example taken on 2 July 2013. At 0521UT, the RBSP-A and GOES-15 spacecraft were on essentially identical L shells ($L \sim 7.1$) according to the T89 model. From the model comparison we could estimate the B_o/B values for the two spacecraft. At 0521UT, the RBSP $B_{\text{equatorial}}$ value to the measured local B field strength (see Figure A4b) was $B_o/B = 0.49$. The corresponding B_o/B value for GOES-15 was $= 0.87$. Figure A4c shows the MagEIS ($E > 0.8$ MeV) flux versus pitch angle values as red crosses and the GOES $E > 0.8$ MeV flux (near the center of its dynamic pitch angle response function at this time) as the blue cross. This analysis shows a “butterfly” distribution, suggesting that fluxes for electrons mirroring at locations off the equator were higher than those mirroring at the equator.

Figure A4d shows pitch angle analysis for $E > 2$ MeV electrons also at 0521 UT on 2 July 2013. An even stronger tendency toward a butterfly pitch angle distribution is evident. Thus, for such cases, the GOES-15 measurements would produce relatively low flux estimates at a given L value compared to the more complete

pitch angle picture provided by RBSP sensors. This is another factor to consider when assessing daily average comparisons between GOES and RBSP.

Acknowledgments

The authors gratefully acknowledge collaborators in the NASA and NOAA programs that have made available the data sets used in this study. This work was supported by JHU/APL Contract 967399 under NASA's prime contract NAS5-01072. All Van Allen Probes data used are publicly available online (<http://www.rbsep-ect.lanl.gov>). GOES data access are online (<https://www.ngdc.noaa.gov/stp/satellite/goes/dataaccess.html>).

References

Ackerman, S. A., Platnick, S., Bhartia, P. K., Duncan, B., L'Ecuyer, T., Heidinger, A., et al. (2019). *Satellites see the world's atmosphere* (Vol. 59). Boston, MA: American Meteorological Society, Meteorological Monographs. <https://doi.org/10.1175/AMSMONOGRAPHIS-D-18-0009.1>, published online: 2 April, 2019.

Baker, D. N., Blake, J. B., Klebesadel, R. W., & Higbie, P. R. (1986). Highly relativistic electrons in the Earth's outer magnetosphere: 1. Lifetimes and temporal history 1979–1984. *Journal of Geophysical Research*, *91*(A4), 4265–4276. <https://doi.org/10.1029/JA091iA04p04265>

Baker, D. N., Hoxie, V., Zhao, H., Jaynes, A. N., Kanekal, S., Li, X., & Elkington, S. (2019). Multi-year measurements of radiation belt electrons: Acceleration, transport, and loss. *Journal of Geophysical Research: Space Physics*, *124*, 2018JA026259. <https://doi.org/10.1029/2018JA026259>

Baker, D. N., Jaynes, A. N., Hoxie, V. C., Thorne, R. M., Foster, J. C., Li, X., et al. (2014). An impenetrable barrier to ultra-relativistic electrons in the Van Allen Radiation Belt. *Nature*, *515*(7528), 531–534. <https://doi.org/10.1038/nature13956>

Baker, D. N., Kanekal, S. G., Hoxie, V. C., Batisse, S., Bolton, M., Li, X., et al. (2012). The Relativistic Electron-Proton Telescope (REPT) instrument on board the Radiation Belt Storm Probes (RBSP) spacecraft: Characterization of Earth's radiation belt high-energy particle populations. *Space Science Reviews*, *179*(1–4), 337–381. <https://doi.org/10.1007/s11214-012-9950-9>

Baker, D. N., Kanekal, S. G., Hoxie, V. C., Henderson, M. G., Li, X., Spence, H. E., et al. (2013). A long-lived relativistic electron storage ring embedded within the Earth's outer Van Allen Radiation Zone. *Science*, *340*(6129), 186–190. <https://doi.org/10.1126/science.1233518>

Baker, D. N., & Lanzerotti, L. J. (2016). "Resource Letter" for Space Weather. *Space Weather*, *14*, 528–529. <https://doi.org/10.1002/2016W001485>

Blake, J. B., Carranza, P. A., Claudepierre, S. G., Clemmons, J. H., Crain, W. R., Dotan, Y., et al. (2013). The Magnetic Electron Ion Spectrometer (MagEIS) instruments aboard the Radiation Belt Storm Probes (RBSP) spacecraft. *Space Science Reviews*, *179*(1–4), 383–421. <https://doi.org/10.1007/s11214-013-9991-8>

Fennell, J. F., Claudepierre, S. G., Blake, J. B., O'Brien, T. P., Clemmons, J. H., Baker, D. N., et al. (2015). Van Allen Probes show the inner radiation zone contains no MeV electrons: ECT/MagEIS data. *Geophysical Research Letters*, *42*, 1283–1289. <https://doi.org/10.1002/2014GL062874>

GOES N Series Data Book (2010). Prepared for NASA pursuant to contract NAS5-98069, Revision D.

Hanser, F. A. (2011). *EPS/HEPAD calibration and data handbook*, Tech. Rep. GOESN-ENG-048D, (). Carlisle, MA: Assurance Technology, Corporation. Retrieved from <http://www.ngdc.noaa.gov/stp/satellite/goes/documentation.html>

Li, X., Selesnick, R. A., Baker, D. N., Jaynes, A. N., Kanekal, S. G., Schiller, Q., et al. (2015). Upper limit on the inner radiation belt MeV electron intensity. *Journal of Geophysical Research: Space Physics*, *120*, 1215–1228. <https://doi.org/10.1002/2014JA020777>

Mauk, B. H., Fox, N. J., Kanekal, S. G., Kessel, R. L., Sibeck, D. G., & Ukhorskiy, A. (2013). Science objectives and rationale for the radiation belt storm probes mission. *Space Science Reviews*, *179*, 3–27. <https://doi.org/10.1007/s11214-012-9908-y>

Meredith, N. P., Horne, R. B., Isles, J. D., & Rodriguez, J. V. (2015). Extreme relativistic electron fluxes at geosynchronous orbit: Analysis of GOES E > 2 MeV electrons. *Space Weather*, *13*, 170–184. <https://doi.org/10.1002/2014SW001143>

Morley, S. K., Sullivan, J. P., Henderson, M. G., Blake, J. B., & Baker, D. N. (2016). The Global Positioning System constellation as a space weather monitor: Comparison of electron measurements with Van Allen Probes data. *Space Weather*, *14*, 76–92. <https://doi.org/10.1002/2015SW001339>

Nagai, T. (1987). Field aligned currents associated with substorms in the vicinity of Synchronous orbit. 2. GOES 2 and GOES 3 observations. *Journal of Geophysical Research*, *92*(A3), 2432–2446. <https://doi.org/10.1029/JA092iA03p02432>

Onsager, T. G., Chan, A. A., Fei, Y., Elkington, S. R., Green, J. C., & Singer, H. J. (2004). The radial gradient of relativistic electrons at geosynchronous orbit. *Journal of Geophysical Research*, *109*, A05221. <https://doi.org/10.1029/2003JA010368>

Ozeke, L. G., Mann, I. R., Murphy, K. R., Degeling, A. W., Claudepierre, S. G., & Spence, H. E. (2018). Explaining the apparent impenetrable barrier to ultra-relativistic electrons in the outer Van Allen belts. *Nature Communications*, *9*(1), 1844. <https://doi.org/10.1038/s41467-018-04162-3>

Rodriguez, J. V., Krossschell, J. C., & Green, J. C. (2014). Intercalibration of GOES 8–15 solar proton detectors. *Space Weather*, *12*, 92–109. <https://doi.org/10.1002/2013SW000996>

SILSO (2019). World Data Center—Sunspot number and long-term solar observations, Royal Observatory of Belgium, on-line Sunspot Number Catalogue: <http://www.sidc.be/SILSO/>

Singer, H. J., Hughes, W. J., Gelpi, C., & Ledley, B. G. (1985). Magnetic disturbances in the vicinity of synchronous orbit and the substorm current wedge: A case study. *Journal of Geophysical Research*, *90*(A10), 9583–9589. <https://doi.org/10.1019/JA090iA10p09583>

Singer, H. J., Matheson, L., Grubb, R., Newman, A., & Bouwer, S. D. (1996). Monitoring space weather with the GOES magnetometers. In E. R. Washwell (Ed.), *SPIE Conference Proceedings* (Vol. 2812, pp. 299–308). Bellingham, WA: GOES-8 and Beyond SPIE.

Tsyganenko, N. A. (1989). A Magnetospheric magnetic field model with a warped tail current sheet. *Planetary and Space Science*, *37*(1), 5–20. [https://doi.org/10.1016/0032-0633\(89\)90066-4](https://doi.org/10.1016/0032-0633(89)90066-4)

Thorne, R. M., Li, W., Ni, B., Ma, Q., Bortnik, J., Chen, L., et al. (2013). Rapid local acceleration of relativistic radiation belt electrons by magnetospheric chorus. *Nature*, *504*(7480), 411–414. <https://doi.org/10.1038/nature12889>

Upton, L. A., & Hathaway, D. H. (2018). An updated Solar Cycle 25 prediction with AFT: The modern minimum. *Geophysical Research Letters*, *45*, 8091–8095. <https://doi.org/10.1029/2018BL078387>

Zhao, H., Baker, D. N., Li, X., Jaynes, A. N., & Kanekal, S. G. (2019). The effects of geomagnetic storms and solar wind conditions on the ultrarelativistic electron flux enhancements. *Journal of Geophysical Research: Space Physics*, *124*, 1948–1965. <https://doi.org/10.1029/2018JA026257>